Exclusive vector meson production as a tool to probe QCD low x evolution

Martin Hentschinski
Universidad de las Americas Puebla
Ex-Hacienda Santa Catarina Martir S/N
San Andrés Cholula
72820 Puebla, Mexico
martin.hentschinski@gmail.com

based on:

- I. Bautista, Fernandez Tellez, MH, PRD 94 (2016) 5, 054002, arXiv:1607.05203
- A. Arroyo Garcia, MH, K.Kutak, PLB 795 (2019) 569-575, arXiv:1904.04394
- MH, E. Padron Molina, Phys.Rev.D 103 (2021) 7, 074008, arXiv:2011.02640

10th International Workshop on Charm Physics (CHARM 2020), May 31- June 4, 2021, Mexico City

A process to explore the low x gluon in the proton at the LHC: exclusive photo-production of J/Ψ and $\Psi(2s)$

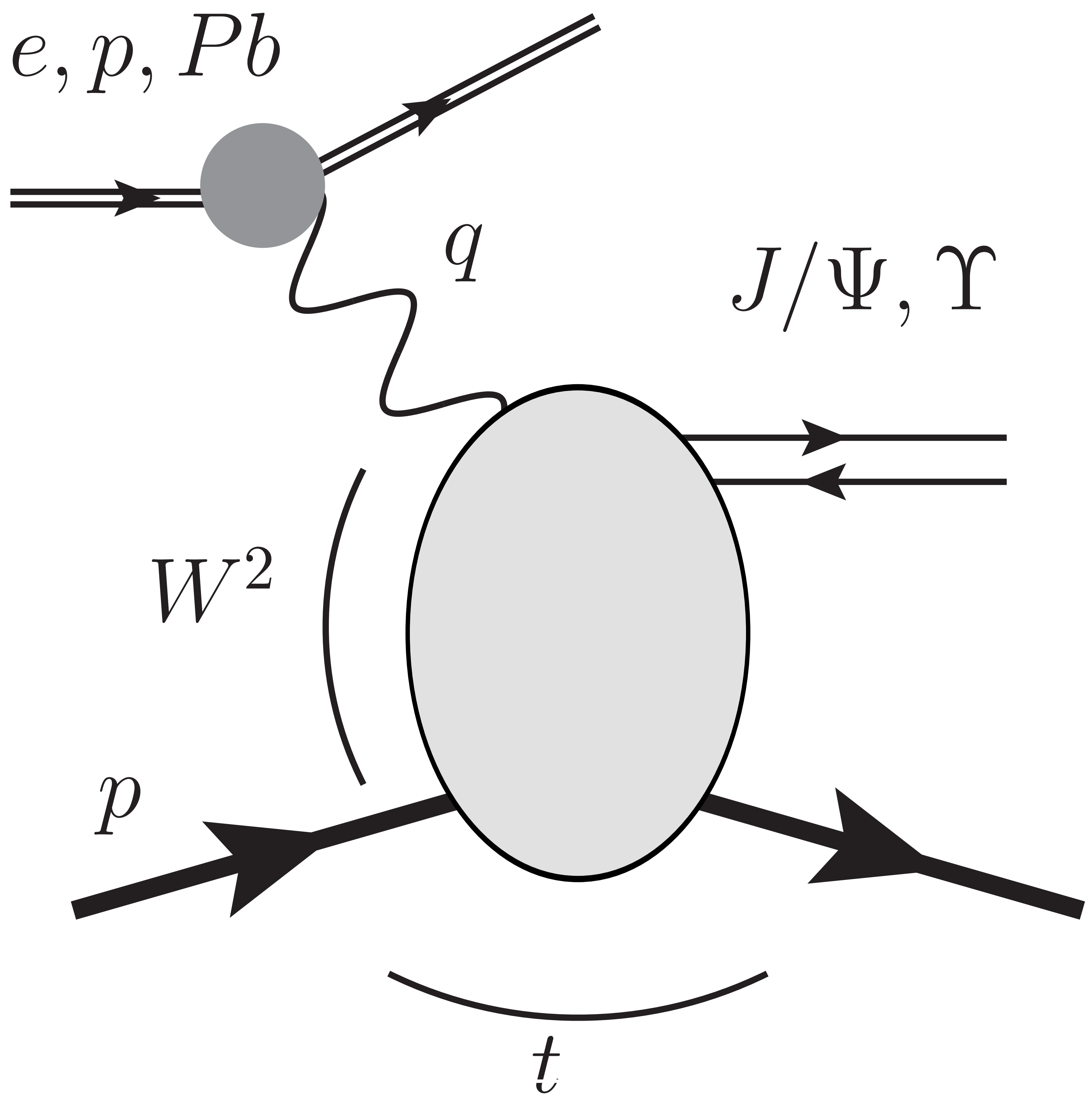

- hard scale: charm mass (small, but perturbative)
- reach up to x≳.5 · 10^{-6}
- perturbative cross-check: ϒ (b-mass)
- measured at **LHC** (LHCb, ALICE, CMS) & **HERA** (H1, ZEUS)

the challenge: describe correctly charmonium production

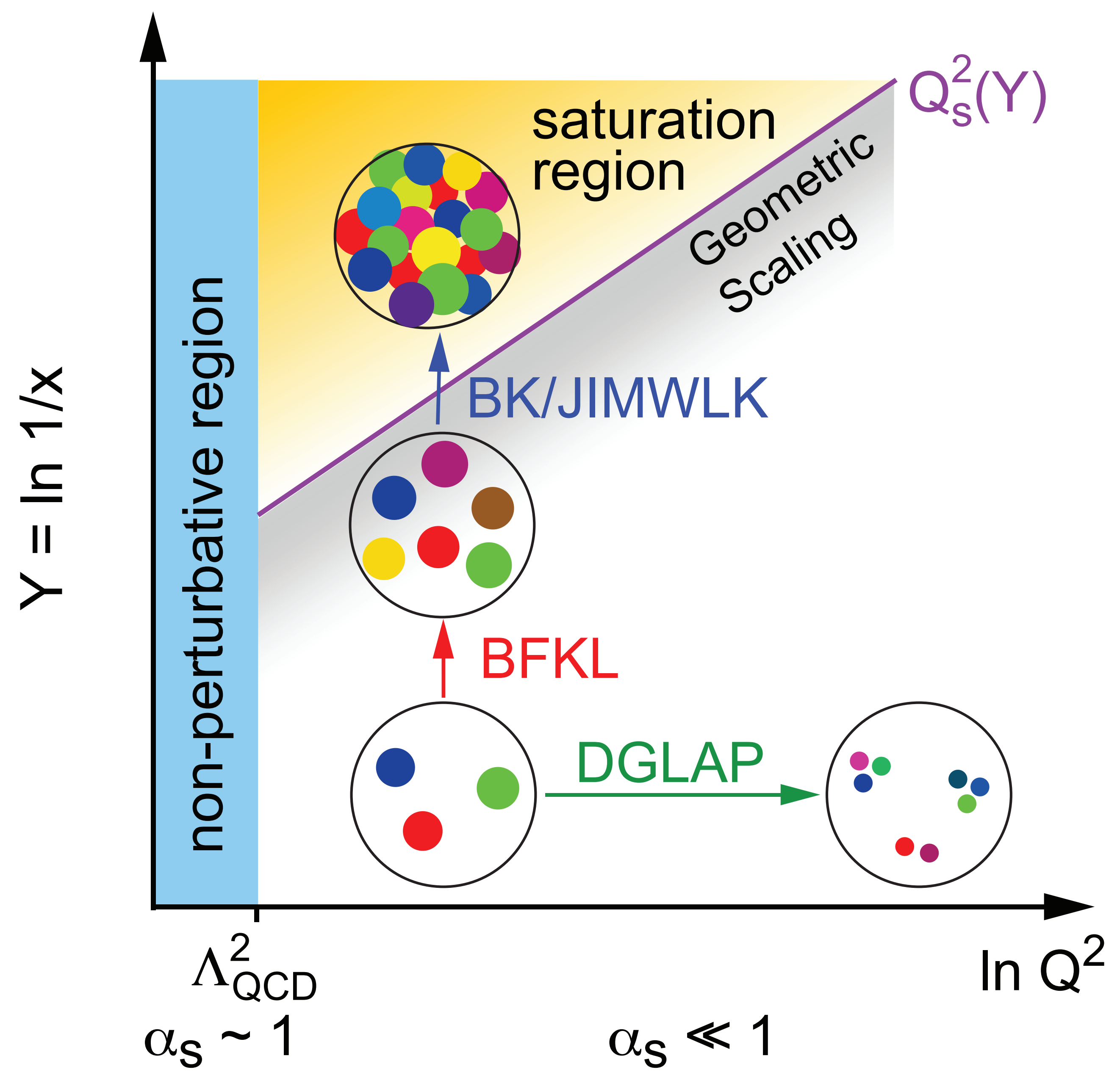

our study:

- instead of DGLAP vs low x
- linear low x (BFKL) vs. non-linear low x (BK)
- failure of BFKL = sign for BK→ high & saturated gluon

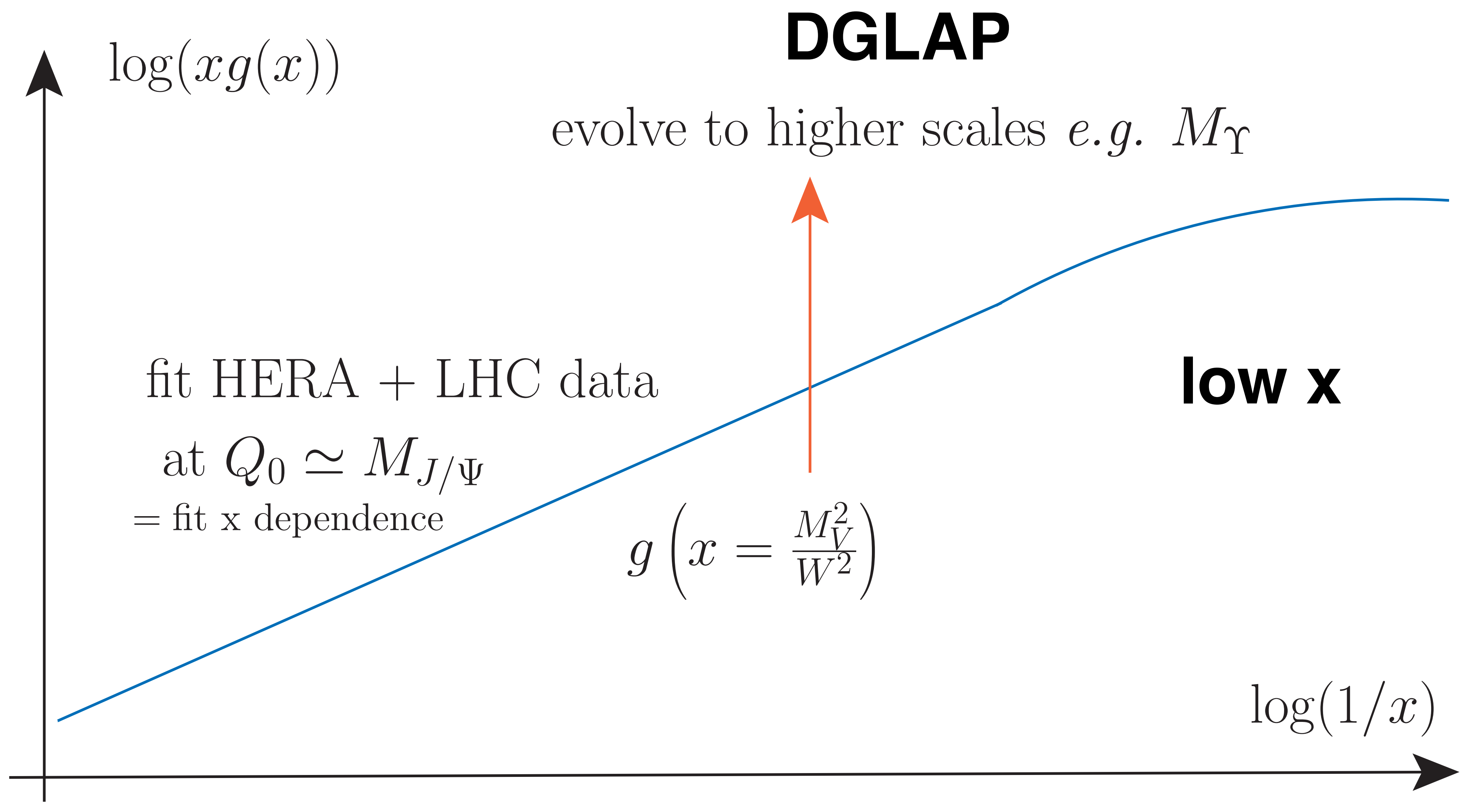

details:

BK evolution for dipole amplitude *N(x,r)*∈ [0,1] [related to gluon distribution]

kernel calculated in pQCD

$$\frac{dN(x,r)}{d\ln\frac{1}{x}} = \int d^2\boldsymbol{r}_1 K(\boldsymbol{r},\boldsymbol{r}_1)\left[N(x,r_1)+N(x,r_2)-N(x,r) - N(x,r_1)N(x,r_2)\right]$$

linear BFKL evolution = subset of complete BK

non-linear term relevant for N~1 (=high density)

linear low x evolution as benchmark →requires precision

(updated version desirable, work has started; not expected too soon)

use: HSS NLO BFKL fit [MH, Salas, Sabio Vera; 1209.1353; 1301.5283]

- uses NLO BFKL kernel

  [Fadin, Lipatov; PLB 429 (1998) 127]

  + resummation of collinear logarithms

- initial kT distribution from fit to combined HERA data

  [H1 & ZEUS collab. 0911.0884]

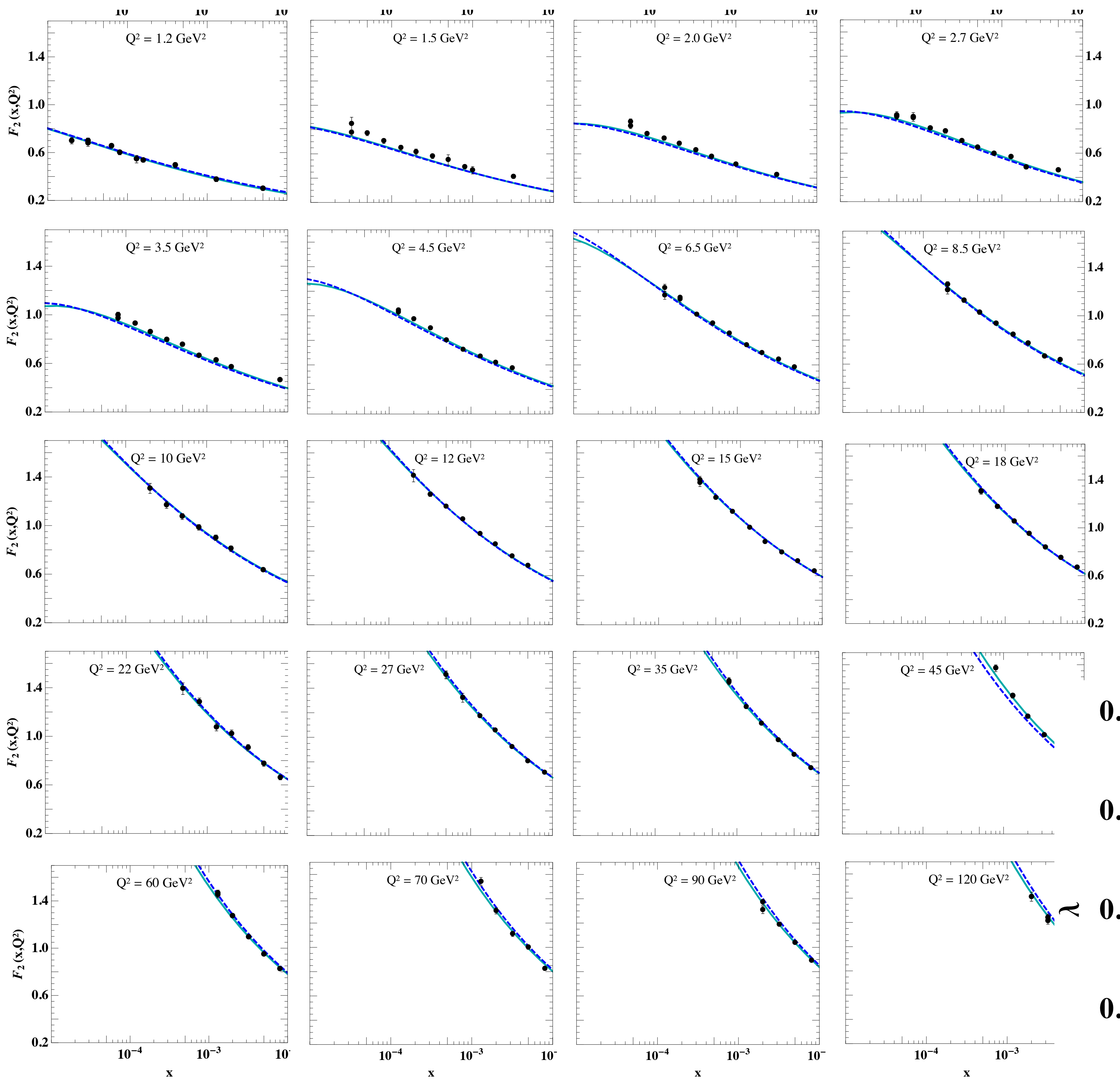

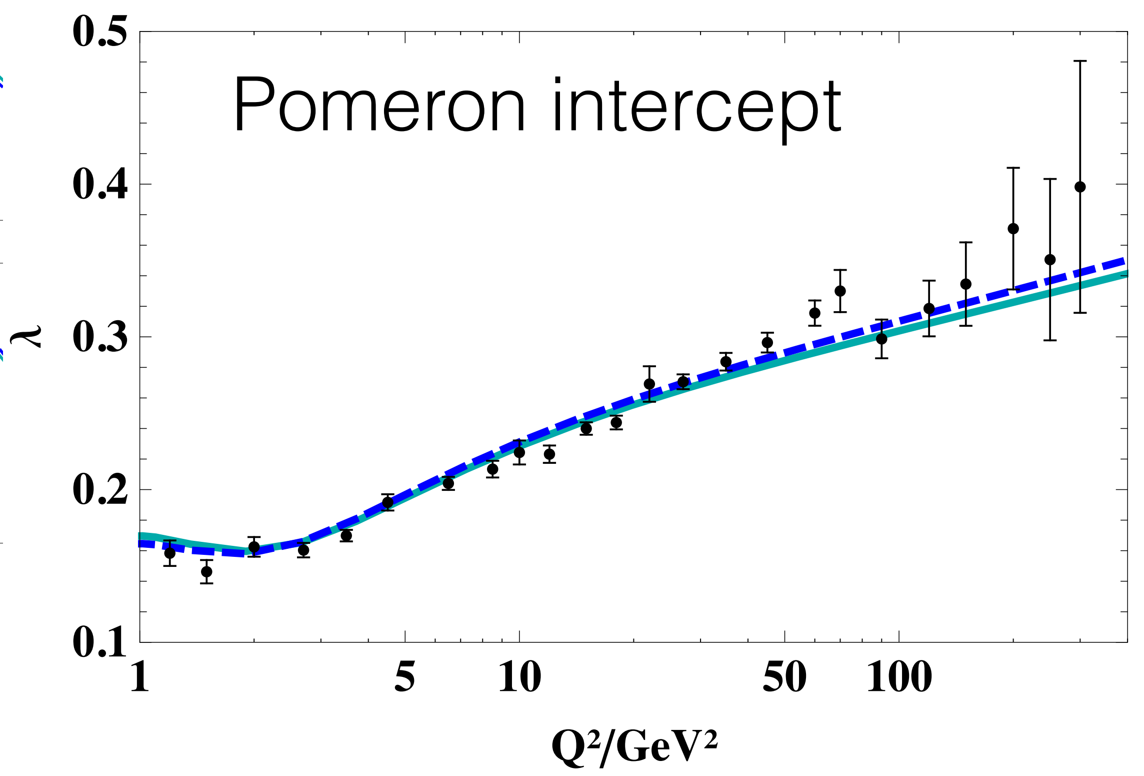

gluon with non-linear terms: KS gluon [Kutak, Sapeta; 1205.5035]

- based on unified (leading order) DGLAP+BFKL framework [Kwiecínski, Martin, Stasto, PRD 56(1997) 3991]
- combined with leading order BK evolution [Kutak, Kwiecinski;hep-ph/0303209][Kutak, Stasto; hep-ph/0408117]
- initial conditions: fit to combined HERA data [H1 & ZEUS collab. 0911.0884]
- both non-linear and linear version available (= non-linearity switched off)

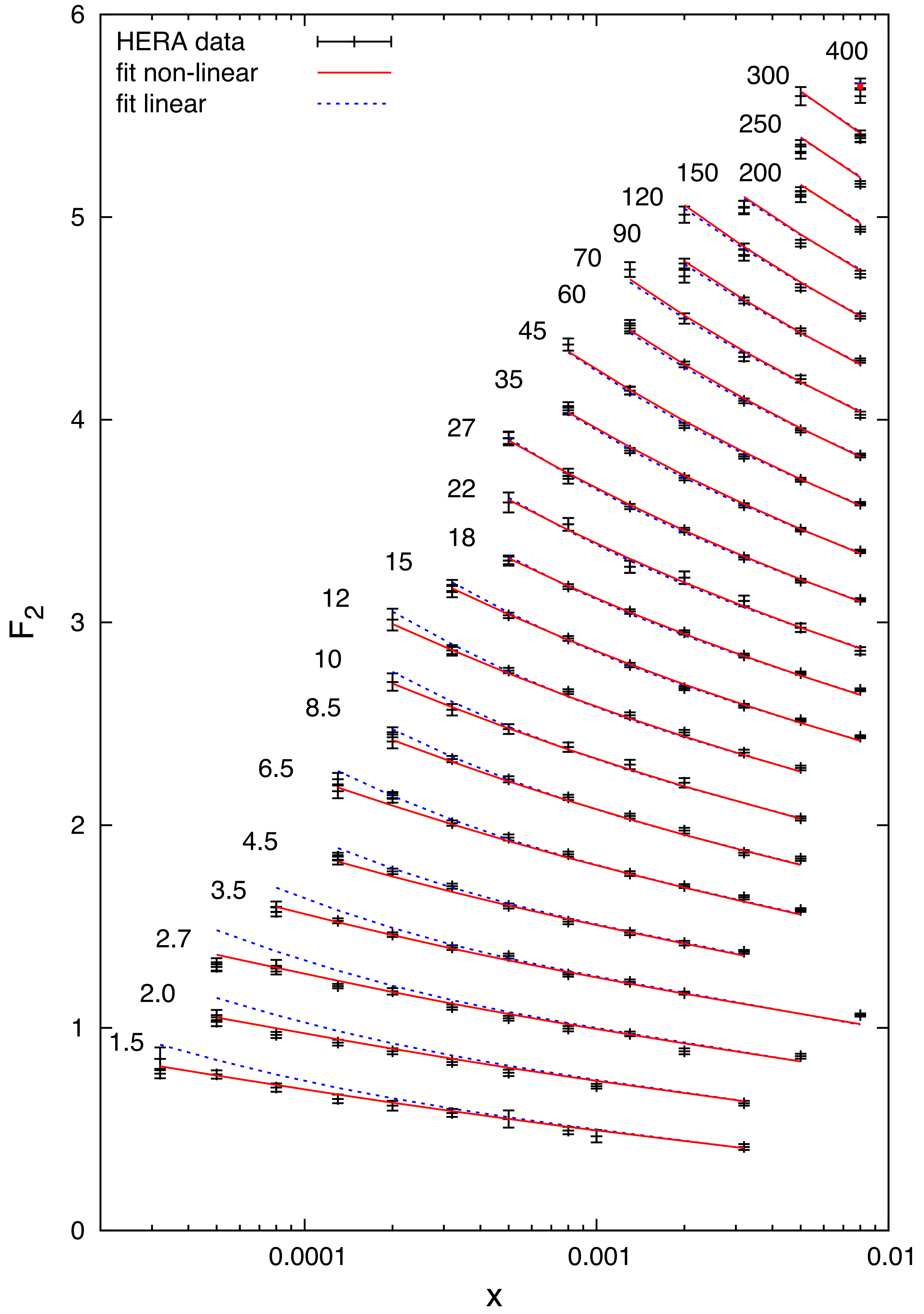

The photo-production Xsection

part I

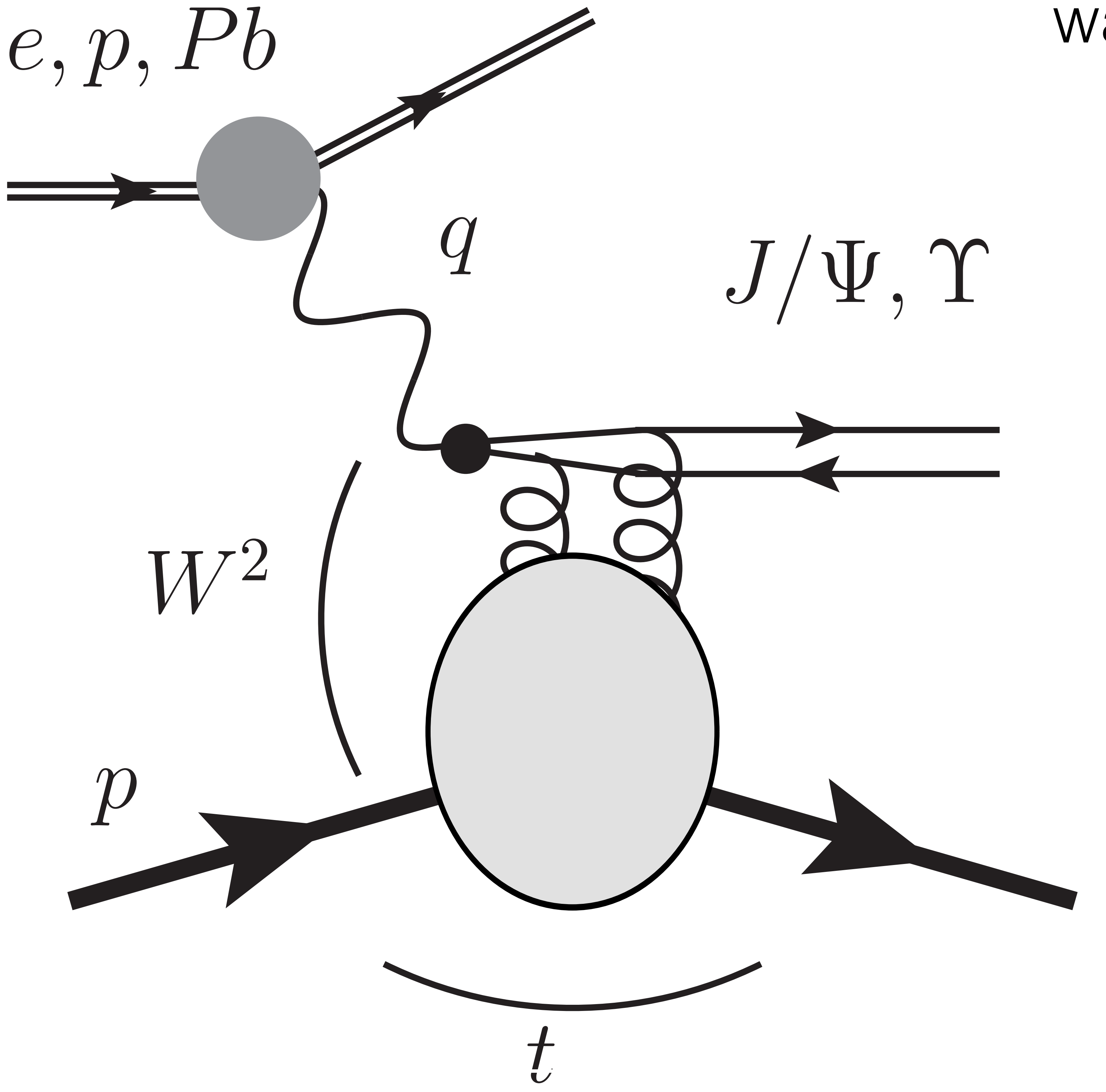

simple approach: Gaussian light-front wave functions [1607.05203, 1904.04394]

$$\Im\mathrm{m}\mathcal{A}^{\gamma p \to V p}(x, t=0) = \int_0^\infty dr W(r) \sigma_{q\bar{q}}(x, r)$$

elements:

r: transverse size of quark-antiquark dipole

$$W(r) = 2\pi r \int_0^1 \frac{dz}{4\pi} (\Psi_V^* \Psi)_T(r, z)$$

integrated light-front wave function overlap = transition photon → dipole → vector meson

$$\sigma_{q\bar{q}}(x, r) = \frac{4\pi}{N_c} \int \frac{d^2\boldsymbol{k}}{\boldsymbol{k}^2} \left(1 - e^{i\boldsymbol{k}\cdot\boldsymbol{r}}\right) \alpha_s \mathcal{F}(x, \boldsymbol{k}^2)$$

explore inclusive gluon → can only calculate imaginary part of scattering amplitude at t=0

= diffraction process

dipole cross-section from unintegrated gluon $\mathscr{F}$
=**object of interest**

how to compare to experiment?

(sort of standard procedure for comparing inclusive gluon to exclusive data)

a) analytic properties of scattering amplitude → real part

$$\mathcal{A}^{\gamma p \to V p}(x, t=0) = \left(i + \tan\frac{\lambda(x)\pi}{2}\right) \cdot \Im\mathrm{m}\mathcal{A}^{\gamma p \to V p}(x, t=0)$$

with intercept

$$\lambda(x) = \frac{d \ln \Im\mathrm{m}\mathcal{A}(x,t)}{d \ln 1/x}.$$

b) differential Xsection at t=0:

$$\frac{d\sigma}{dt}(\gamma p \to V p)\bigg|_{t=0} = \frac{1}{16\pi}\left|\mathcal{A}^{\gamma p \to V p}(W^2, t=0)\right|^2$$

c) from experiment:

$$\frac{d\sigma}{dt}(\gamma p \to V p) = e^{-B_D(W)\cdot|t|} \cdot \frac{d\sigma}{dt}(\gamma p \to V p)\bigg|_{t=0}$$

$$\sigma^{\gamma p \to V p}(W^2) = \frac{1}{B_D(W)}\frac{d\sigma}{dt}(\gamma p \to V p)\bigg|_{t=0}$$

extracted from data

weak energy dependence from slope parameter

$$B_D(W) = \left[b_0 + 4\alpha' \ln\frac{W}{W_0}\right] \mathrm{GeV}^{-2}.$$

First study (BFKL only, also for Υ)

[Bautista, MH, Fernandez-Tellez;1607.05203]

NLO BFKL describes energy dependence, but …..

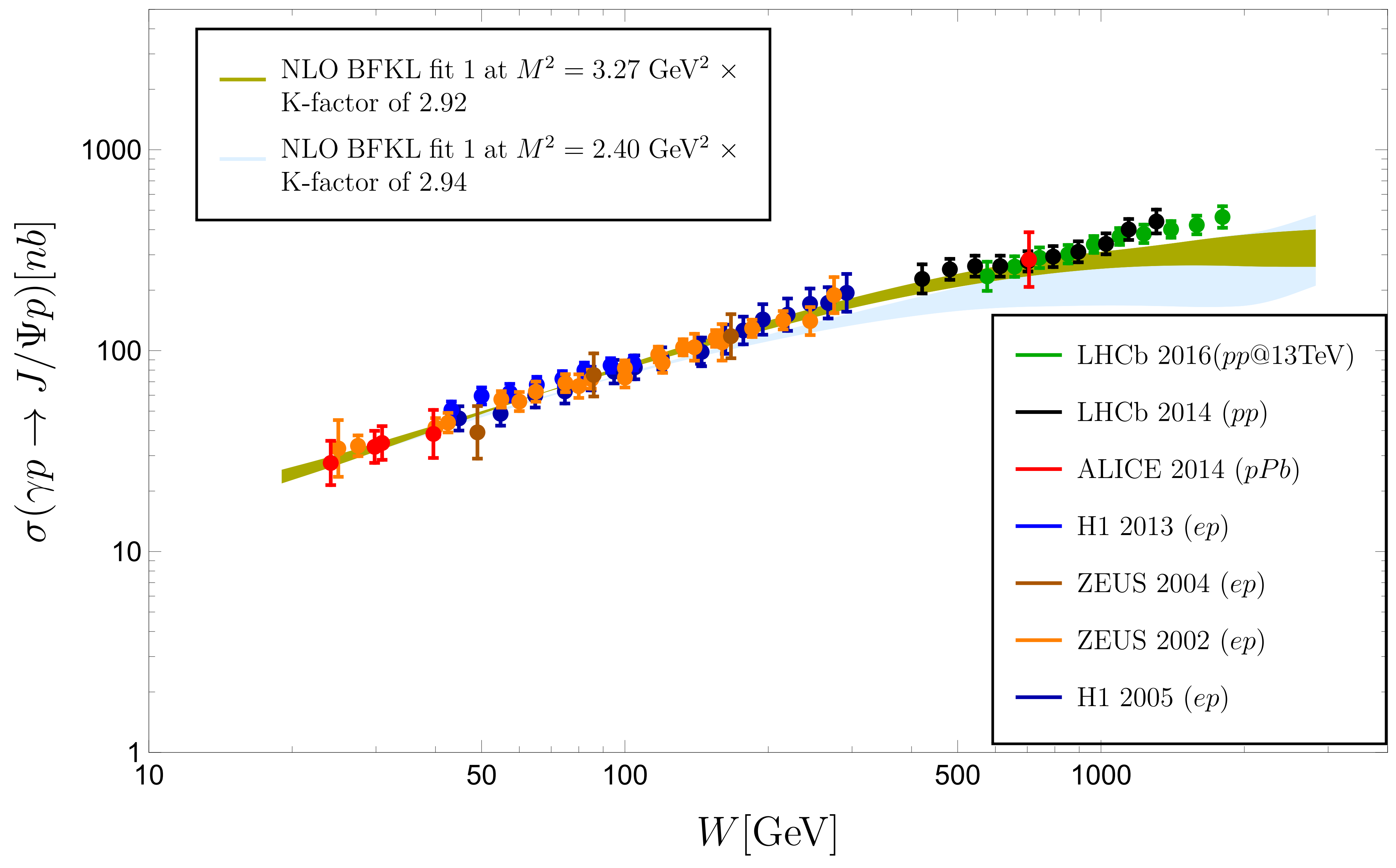

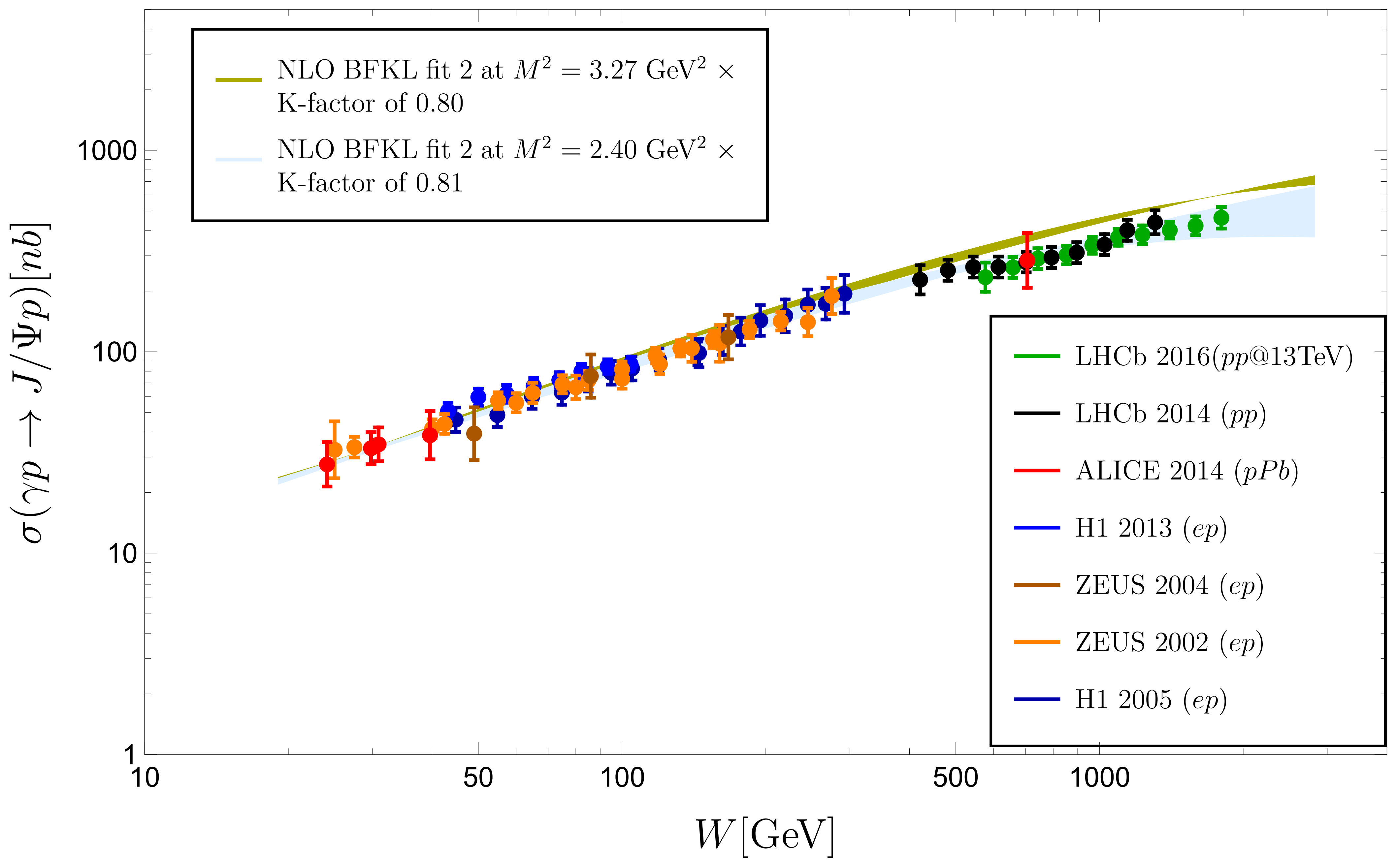

error band: variation of renormalization scale
→ in general pretty small = stability

…but error blows up for highest energies

does it mean something?

Second Study

[Arroyo, MH, Kutak;1904.04394]

- linear vs. nonlinear
- with standard scale choice for NLO BFKL gluon, both distribution describe energy dependence with equal quality

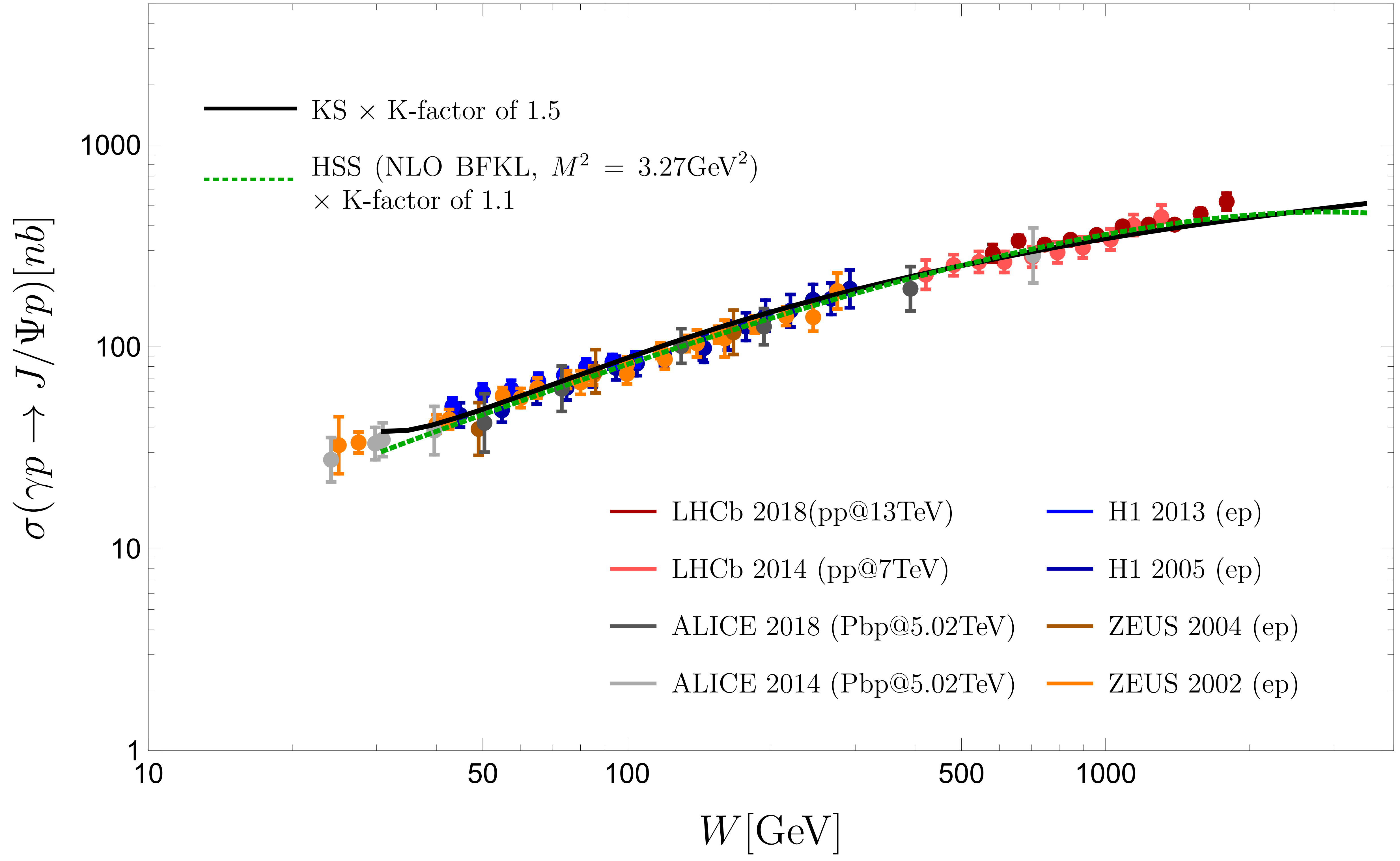

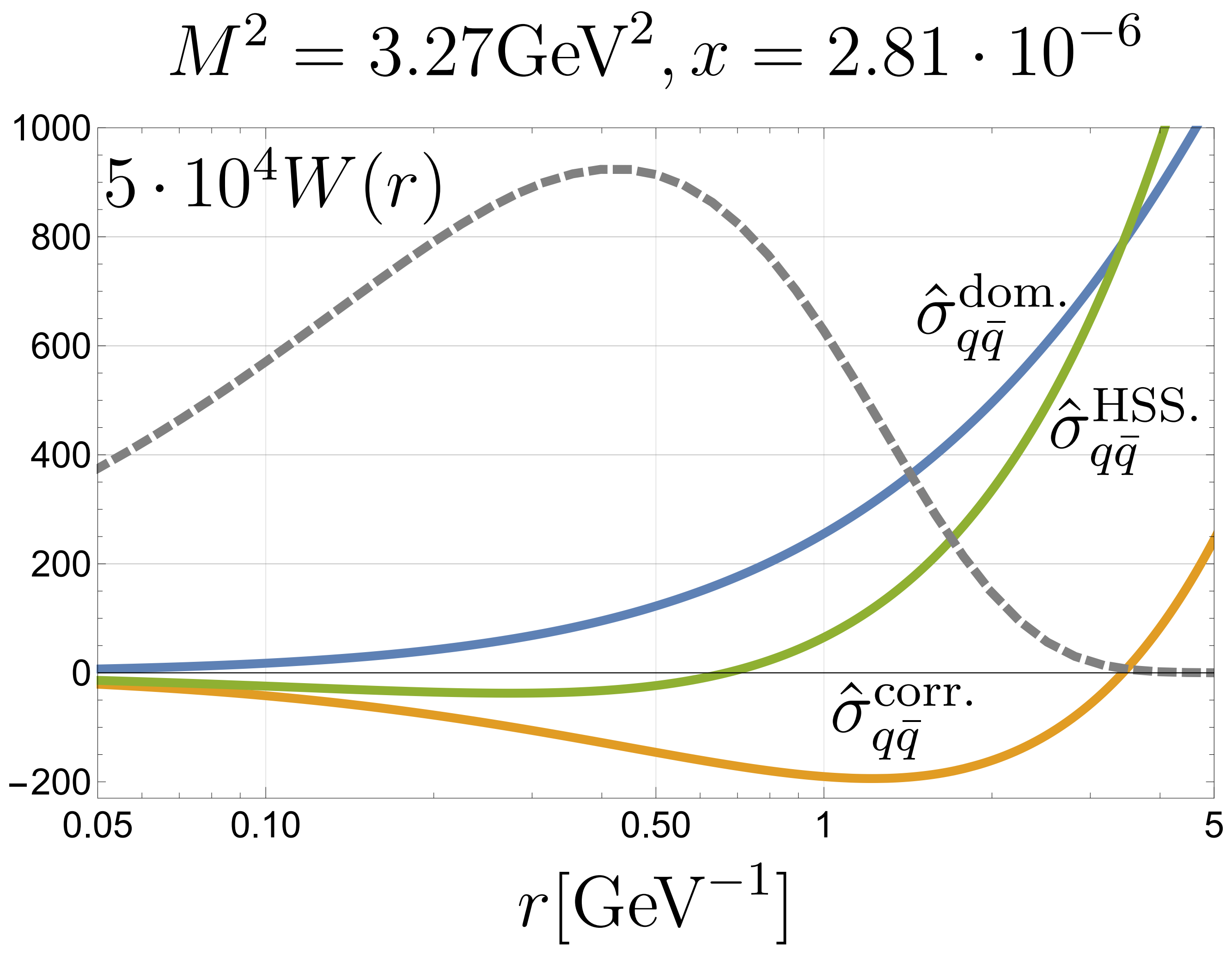

but find:

- with standard scale choice, HSS gluon is unstable for largest energies

$$\hat{\sigma}_{q\bar{q}}^{(\text{HSS})}(x,r) = \hat{\sigma}_{q\bar{q}}^{(\text{dom.})}(x,r) + \hat{\sigma}_{q\bar{q}}^{(\text{corr.})}(x,r),$$

- fix this through dipole size dependent renormalization scale

$$M^2 = \frac{4}{r^2} + \mu_0^2 \text{ with } \mu_0^2 = 1.51 \text{ GeV}^2$$

→ stabilize perturbative expansion through resummation

$$M^2 = \frac{4}{r^2} + \mu_0^2, x = 2.81 \cdot 10^{-6}$$

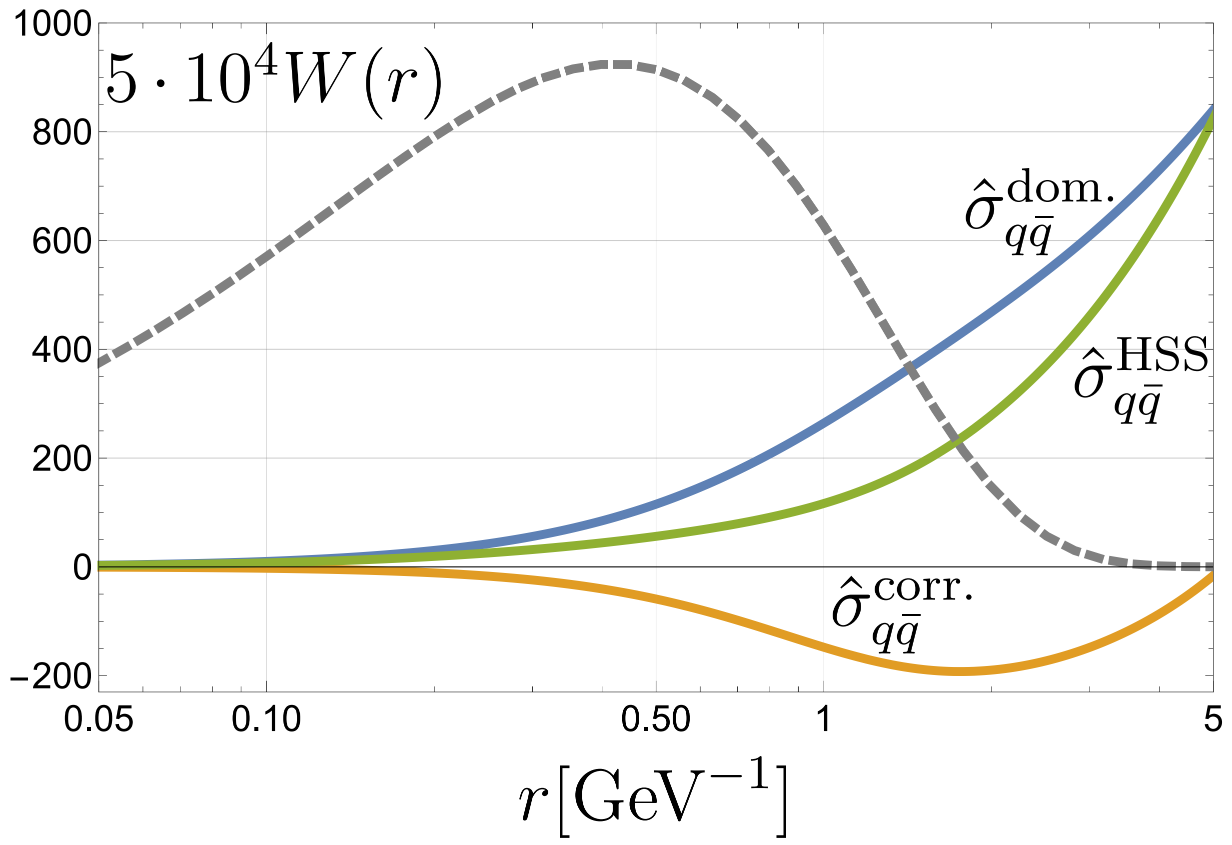

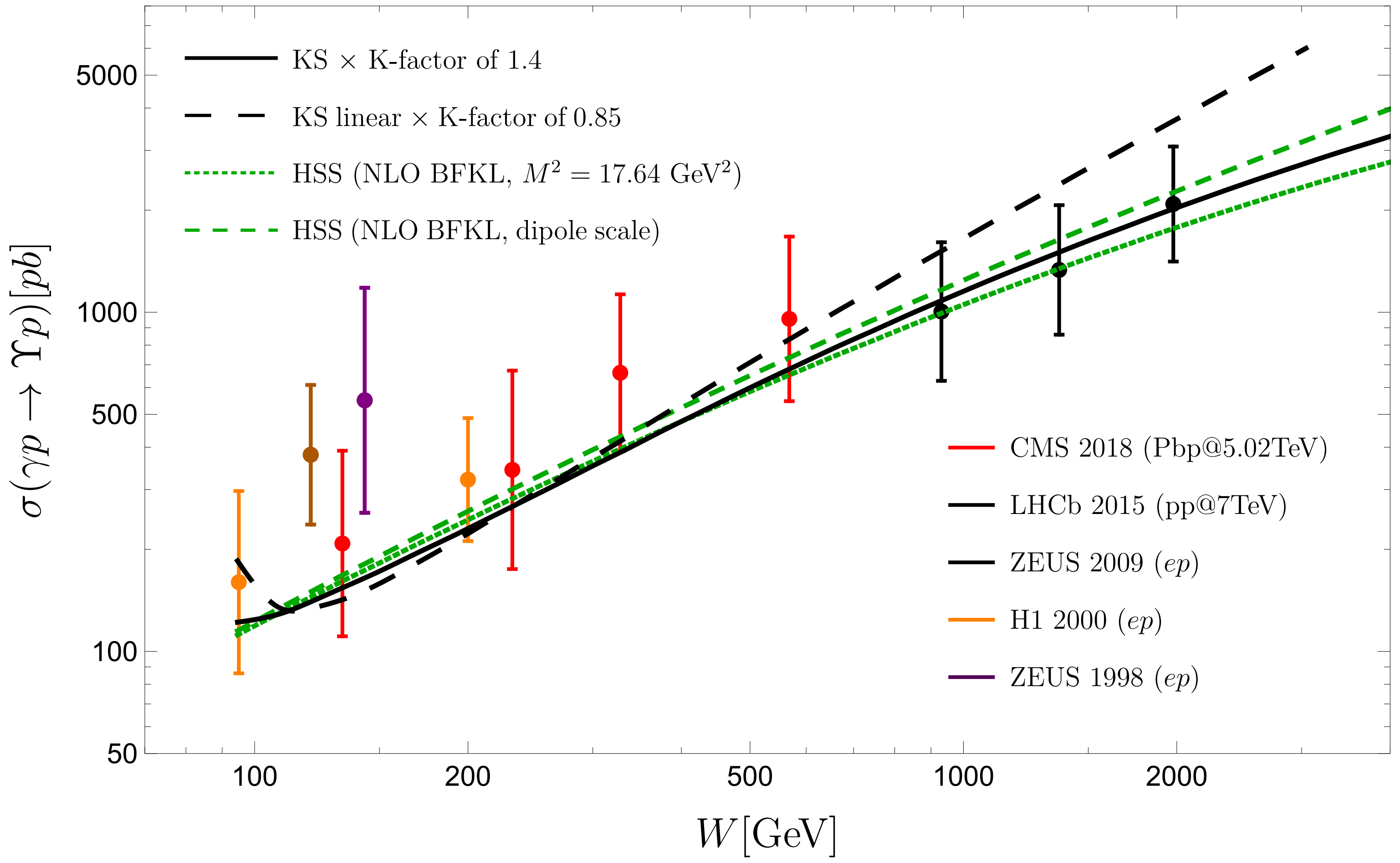

- still describe Υ production
  → perturbative cross-check
- not true for high precision HERA data

stabilizes perturbative expansion → stable NLO BFKL evolution at highest W

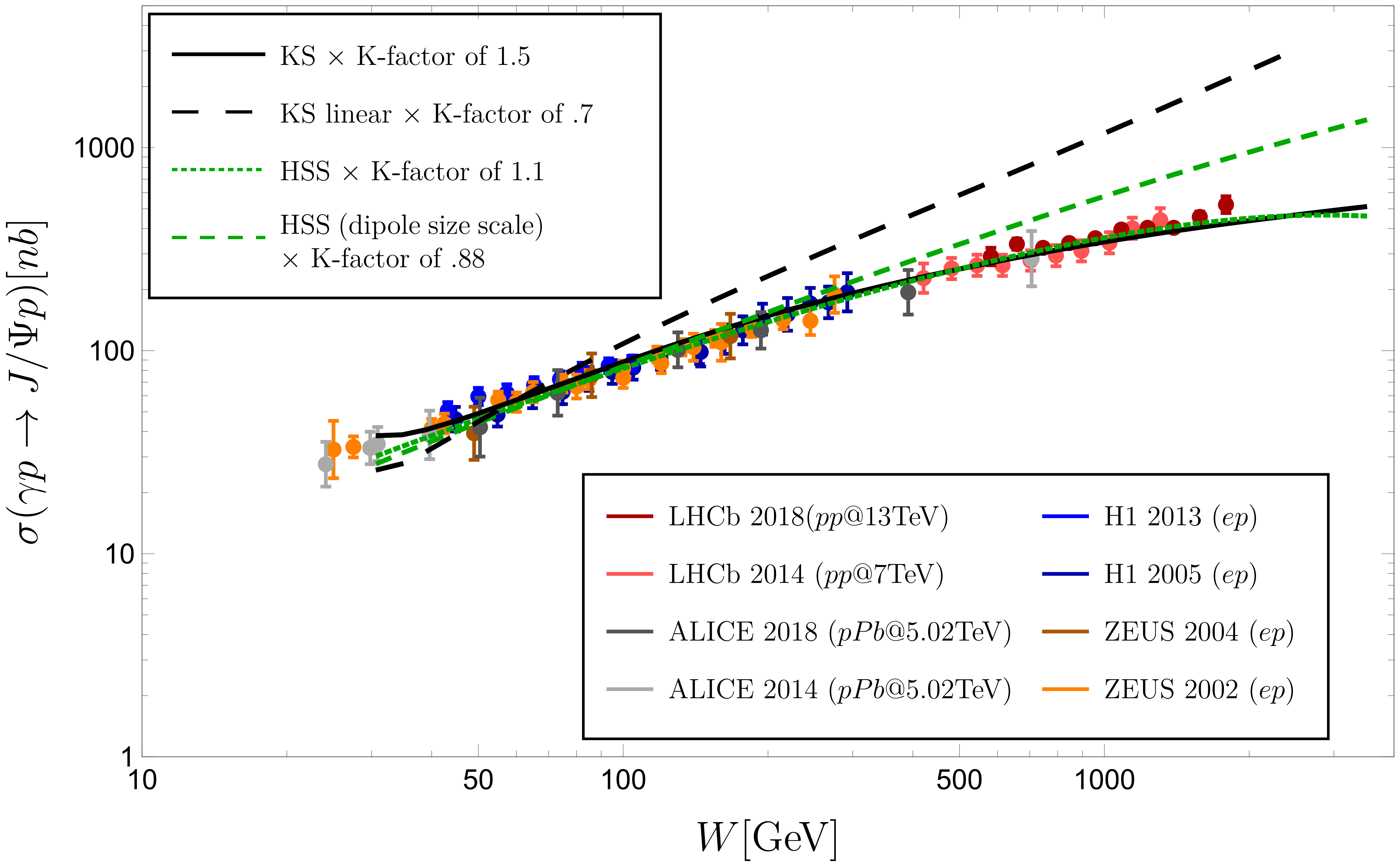

BUT:

- resulting growth too strong for J/Ψ production
- classical sign for onset of high density effects/transition towards saturated regime?

Shortcomings of our 2nd study

- Vector meson wave functions use (conventional) boosted Gaussian model →what about more refined descriptions?
- We do not address excited states $\Psi(2s)$ → different r-shape of the transition due to nodes in the wave function
- refit of NLO BFKL gluon → desirable, but beyond this study; project for future
- estimate uncertainties (scale variation) → how stable is our observation?

Transition amplitude $\gamma \to$ VM

includes relativistic spin rotation effects + (more) realistic $c\bar{c}$ potential both for J/Ψ and $\Psi(2s)$

[Hufner, Y. Ivanov, B. Kopeliovich, A. Tarasov; hep-ph/0007111],
[M. Krelina, J. Nemchik, R. Pasechnik, J. Cepila; 1812.03001; 1901.02664]

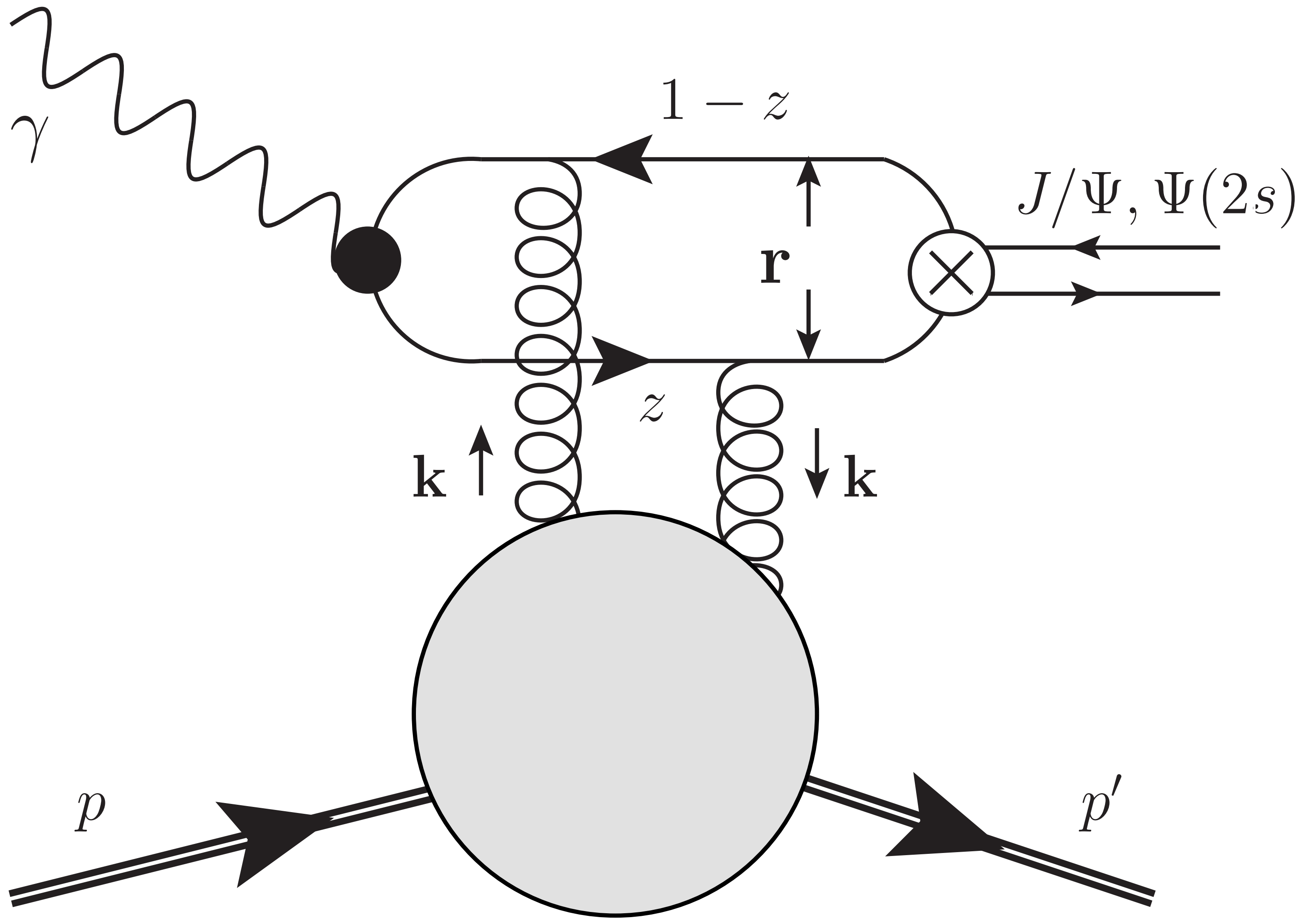

$$\Im\mathrm{m}\mathcal{A}_T(W^2, t=0) = \int d^2\boldsymbol{r} \left[\sigma_{q\bar{q}}\left(\frac{M_V^2}{W^2}, r\right) \Sigma_T^{(1)}(r) + \frac{d\sigma_{q\bar{q}}\left(\frac{M_V^2}{W^2}, r\right)}{dr} \Sigma_T^{(2)}(r) \right]$$

- depends both on dipole cross-section and its derivative
- wave functions have been obtained in [M. Krelina, J. Nemchik, R. Pasechnik, J. Cepila; 1812.03001; 1901.02664] through numerical solution to corresponding Schrödinger equation
- transition function factorizes for real photon ($Q = 0$)
- problem: need boosted wave function

$$\Sigma_T^{(i)}(r) = \hat{e}_f \sqrt{\frac{\alpha_{e.m.} N_c}{2\pi^2}} K_0(m_f r)\, \Xi^{(i)}(r), \qquad i = 1, 2$$

$$\Xi^{(1)}(r) = \int_0^1 dz \int \frac{d^2\boldsymbol{p}}{2\pi} e^{i\boldsymbol{p}\cdot\boldsymbol{r}} \frac{m_T^2 + m_T m_L - 2p_T^2 z(1-z)}{m_T + m_L} \Psi_V(z, |\boldsymbol{p}|),$$

$$\Xi^{(2)}(r) = \int_0^1 dz \int \frac{d^2\boldsymbol{p}}{2\pi} e^{i\boldsymbol{p}\cdot\boldsymbol{r}} |\boldsymbol{p}| \frac{m_T^2 + m_T m_L - 2\boldsymbol{p}^2 z(1-z)}{2m_T(m_T + m_L)} \Psi_V(z, |\boldsymbol{p}|),$$

- $\Psi_V(z, \mathbf{p})$ provided as table by authors of [1812.03001; 1901.02664]
- $m_T^2 = m_f^2 + \boldsymbol{p}^2$, $m_L^2 = 4m_f^2 z(1-z)$,

potentials for wave functions:

as implemented in [M. Krelina, J. Nemchik, R. Pasechnik, J. Cepila; 1812.03001; 1901.02664]

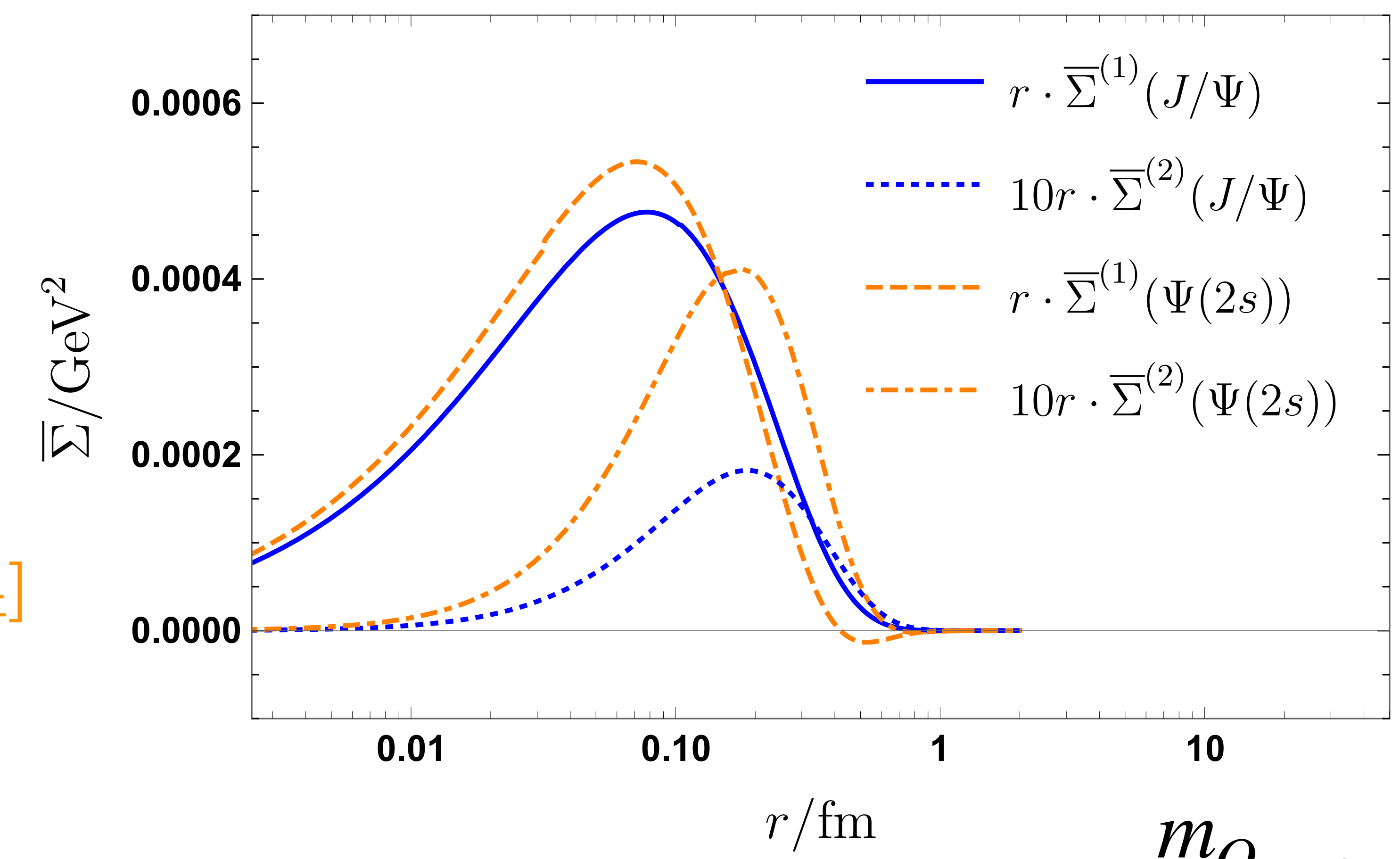

harmonic oscillator (HO): $U(r) = \frac{m_Q}{2}\omega^2 r^2$

$\omega = 0.3$GeV→ Gaussian shape

Note:
- plots show transition function $\gamma \to VM$, not wave function
- $\Psi(2s)$: node structure of wave function absent in transition after integration over photon momentum fraction z
- $\overline{\Sigma}^{(2)}(r)$ enhanced for $\Psi(2s)$, but still considerable smaller

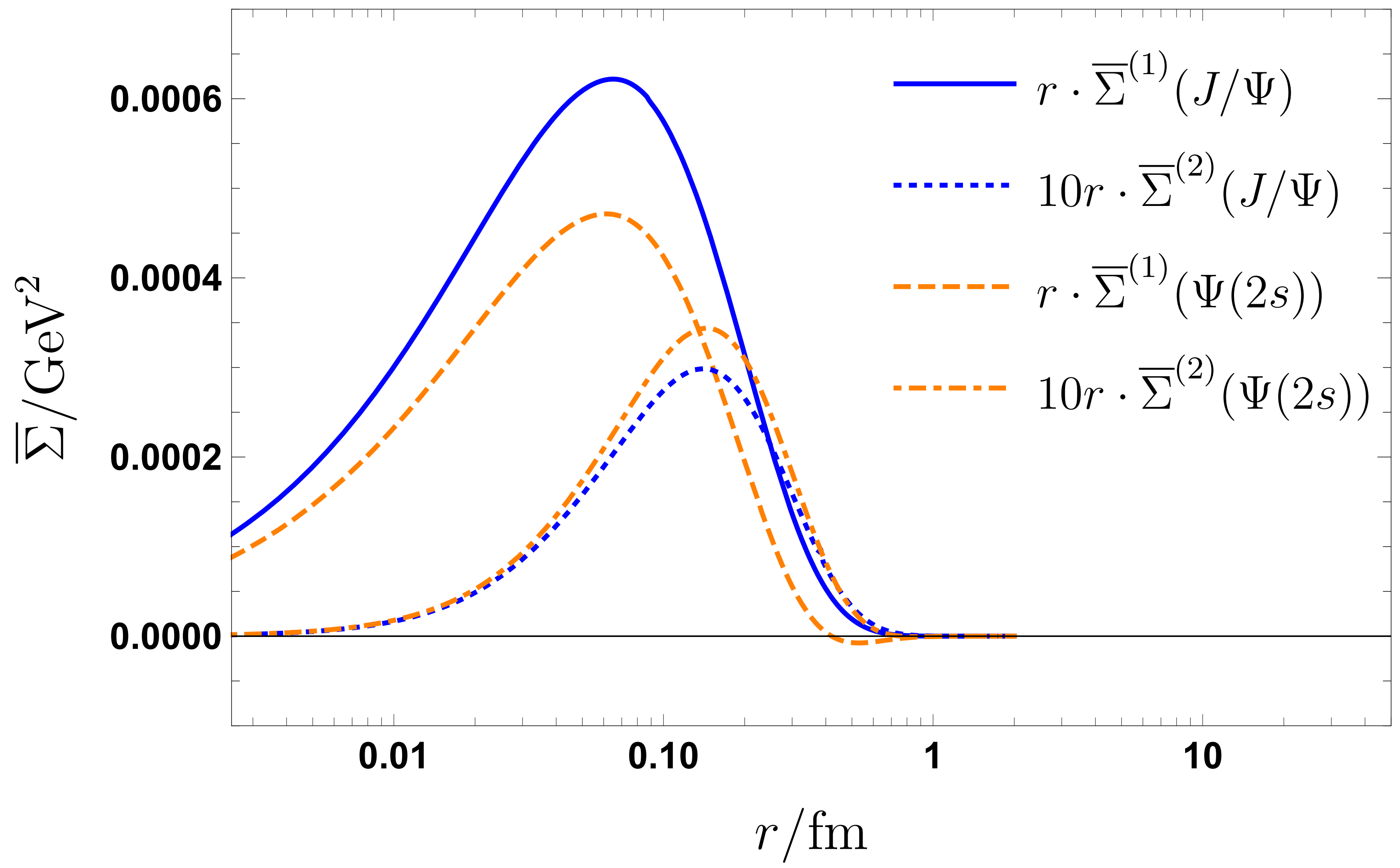

Buchmüller-Tye Potential: Coulomb-like behavior at small r and a string-like behavior at large r [Buchmüller, Tye; PRD24, 132 (1981)]

→$\Psi(2s)$ gives access to a (slightly) different region in r than J/Ψ

→ requires separate diffractive slopes $B_D(W)$ as obtained in [M. Krelina, J. Nemchik, R. Pasechnik, J. Cepila; 1812.03001; 1901.02664]

Buchmüller-Tye potential

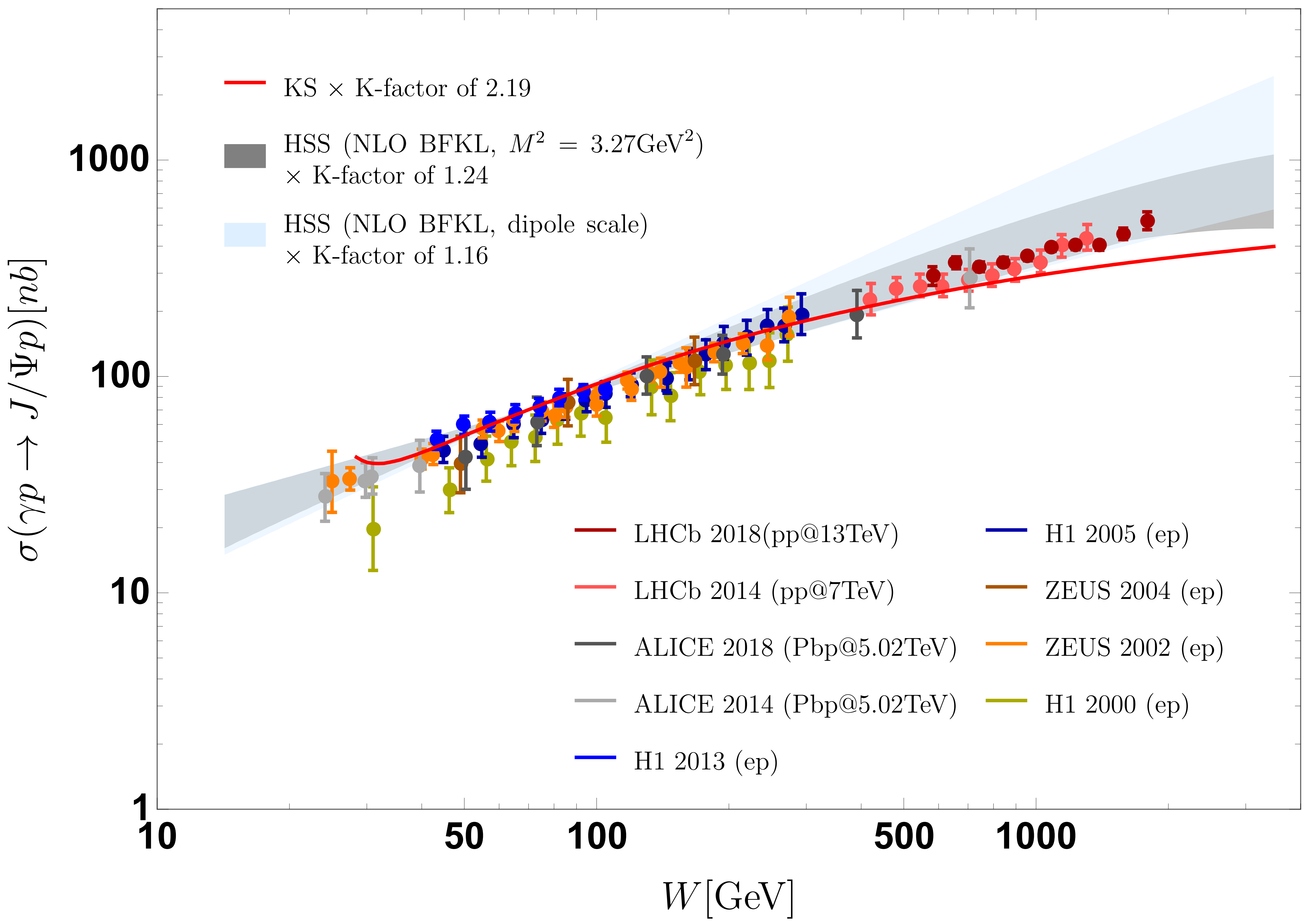

Harmonic Oscillator potential

J/Ψ

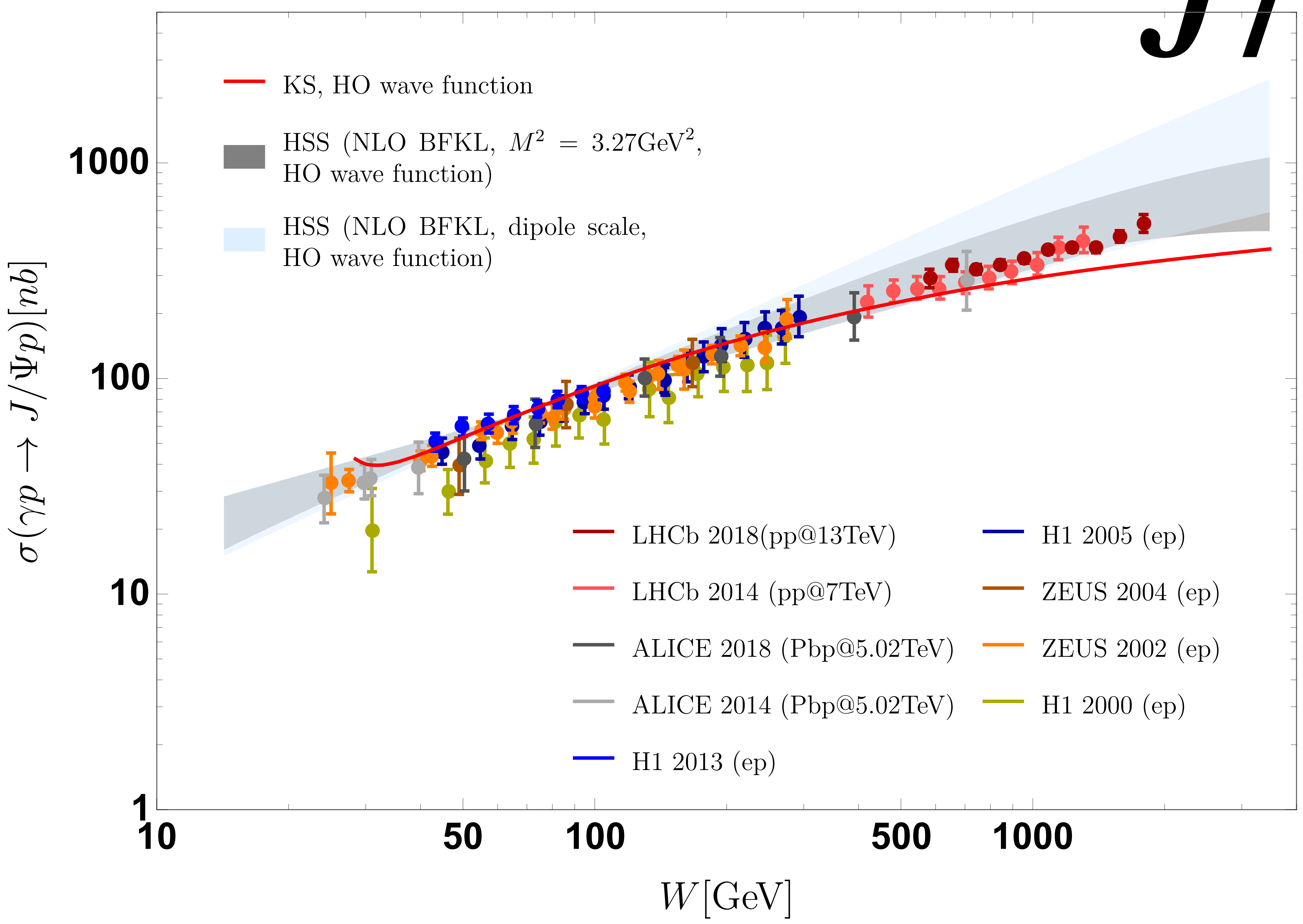

- Fix normalization with low energy data point (HERA); offset in normalization also seen in [M. Krelina, J. Nemchik, R. Pasechnik, J. Cepila; 1812.03001; 1901.02664]
- Uncertainty band = variation of renormalization scale $\bar{M} \in [M/\sqrt{2}, M\sqrt{2}]$
- Difference between linear & non-linear persists, but scale uncertainty too large to distinguish them clearly

$\Psi(2s)$

Buchmüller-Tye potential

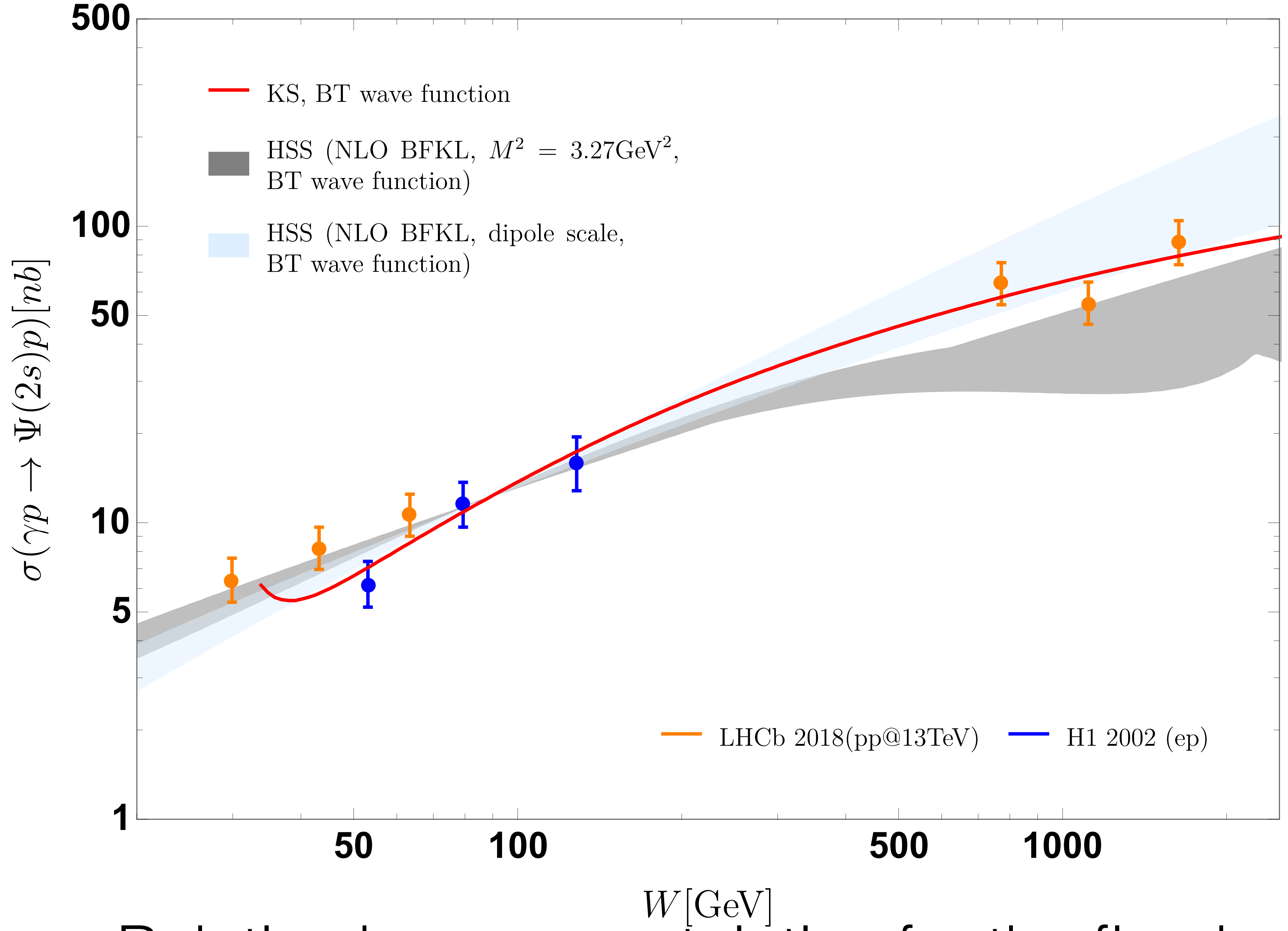

Harmonic Oscillator potential

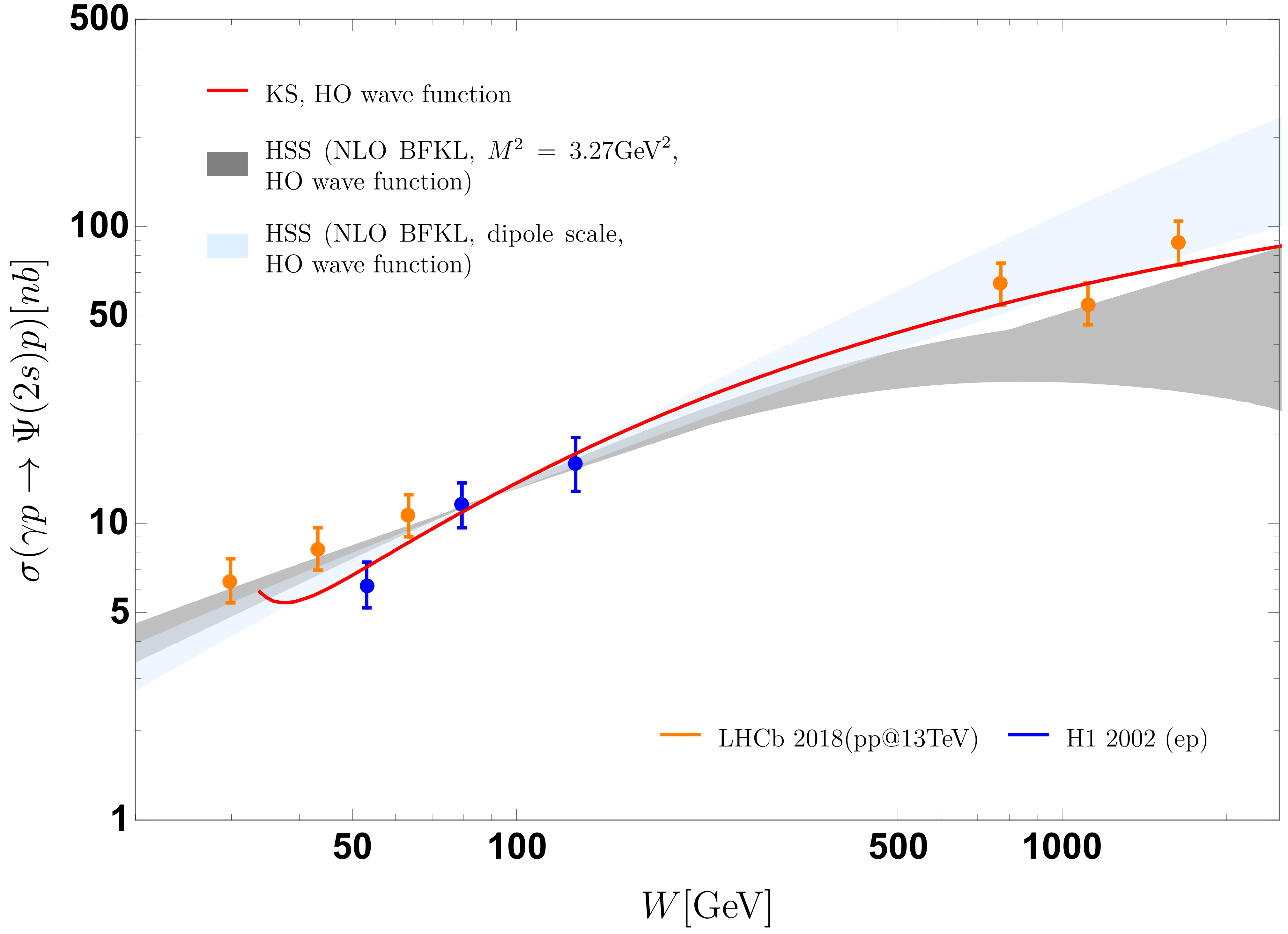

- Relative large uncertainties for the fixed scale HSS (NLO BFKL) gluon →BFKL dipole + node structure;
- stabilized BFKL and non-linear evolution appear closer than for J/Ψ [M. Krelina, J. Nemchik, R. Pasechnik, J. Cepila; 1812.03001; 1901.02664] steeper (perturbative) energy dependence for $\Psi(2s)$ →attributed to reduced cancellation below and above $\Psi(2s)$ node at higher energies

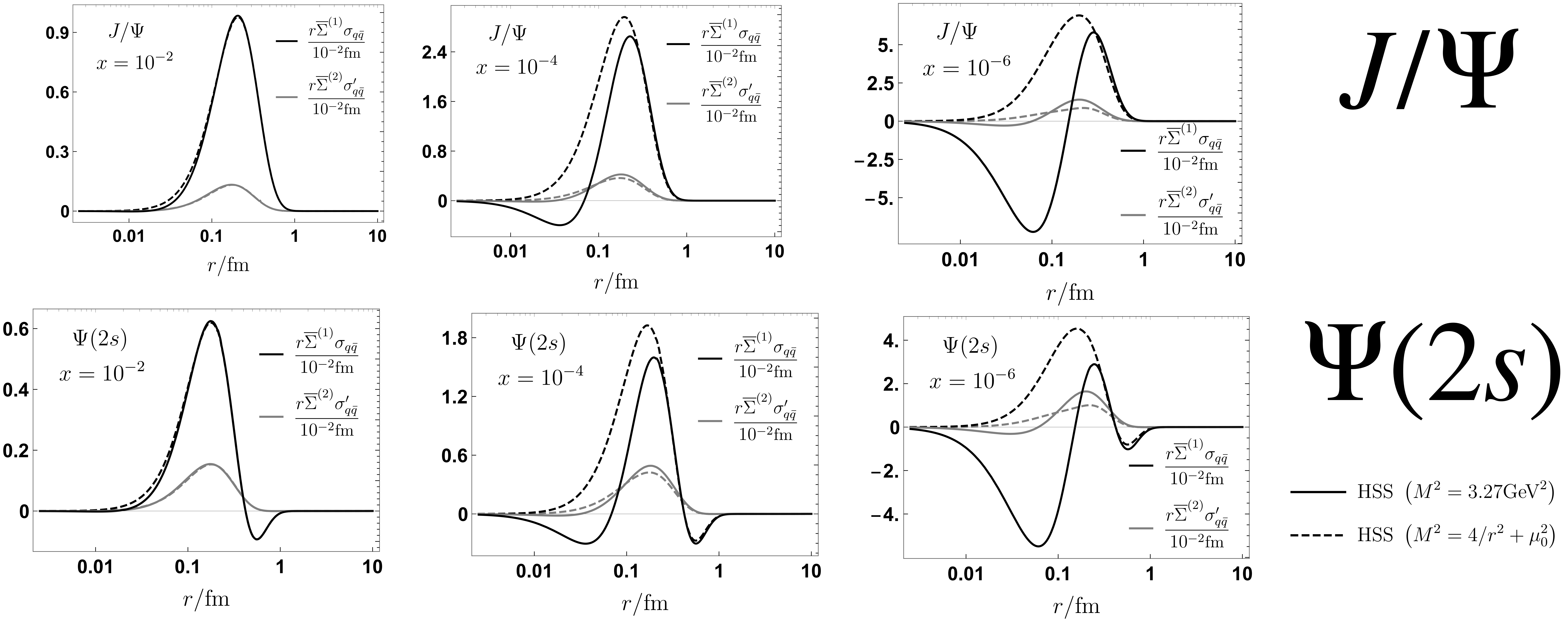

- in both cases the fixed scale dipole develops a negative region with decreasing x
- $\Psi(2s)$: node structure of wave function does not allow to compensate for it → instability

advantage: $\Psi(2s)$ challenges our dipole cross-sections

More interesting: the ratio $\sigma[\Psi(2s)]/\sigma[J/\Psi]$

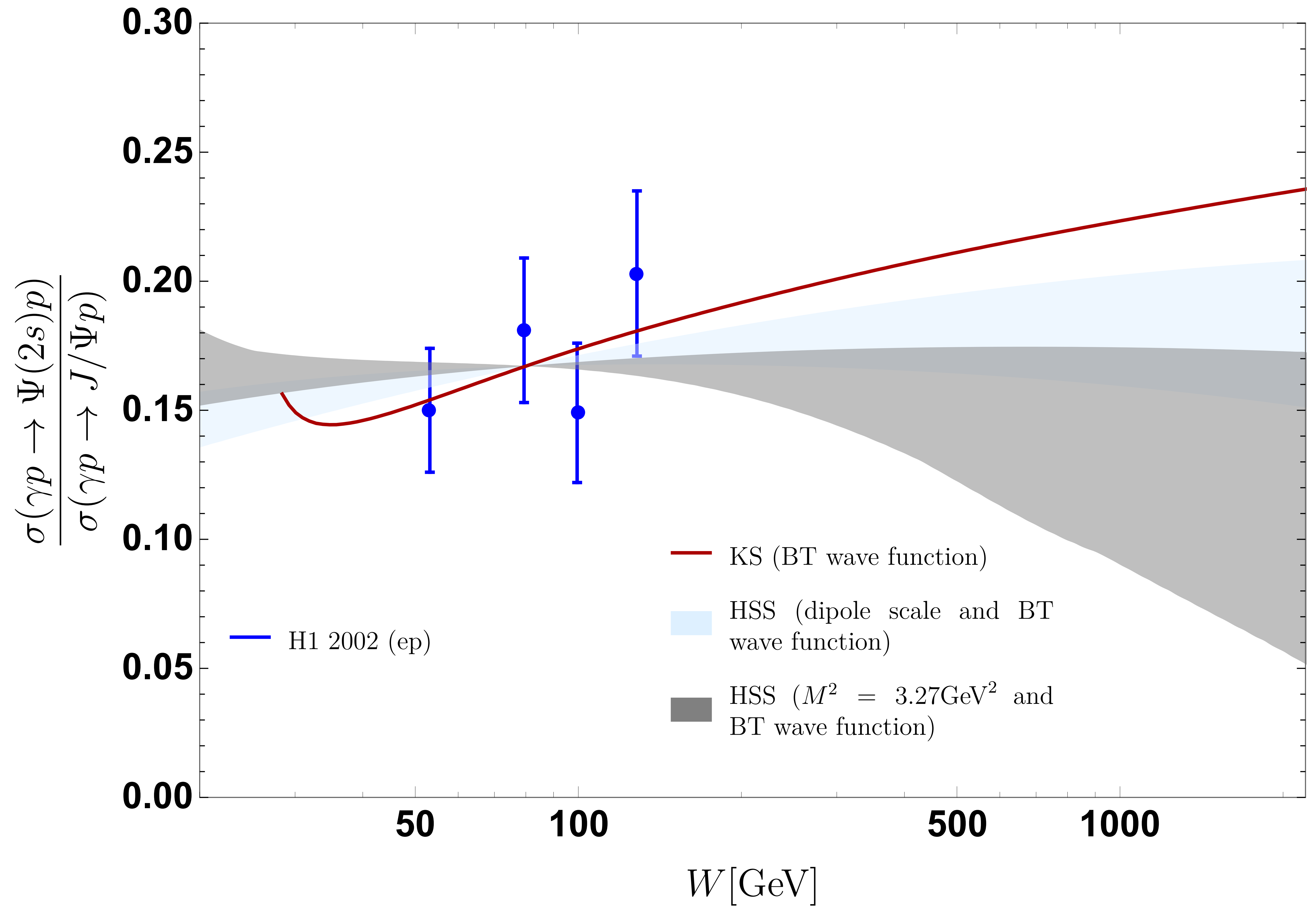

problem: no data at high energies

(J/Ψ and $\Psi(2s)$) LHCb data in different W-bins)

- rise of non-linear gluon also observed in [M. Krelina, J. Nemchik, R. Pasechnik, J. Cepila; 1812.03001; 1901.02664] →KST dipole X-section [Kopeliovich, Schäfer, Tarasov, hep-ph/9908245]
- here: confirmed for KS (BK) gluon
- rise is not present for HSS (NLO BFKL) gluon (stabilized version)
- both slope & curvature differ
- general feature of perturbative QCD evolution?
- Hope: a tool to distinguish linear vs. non-linear evolution?

Conclusions:

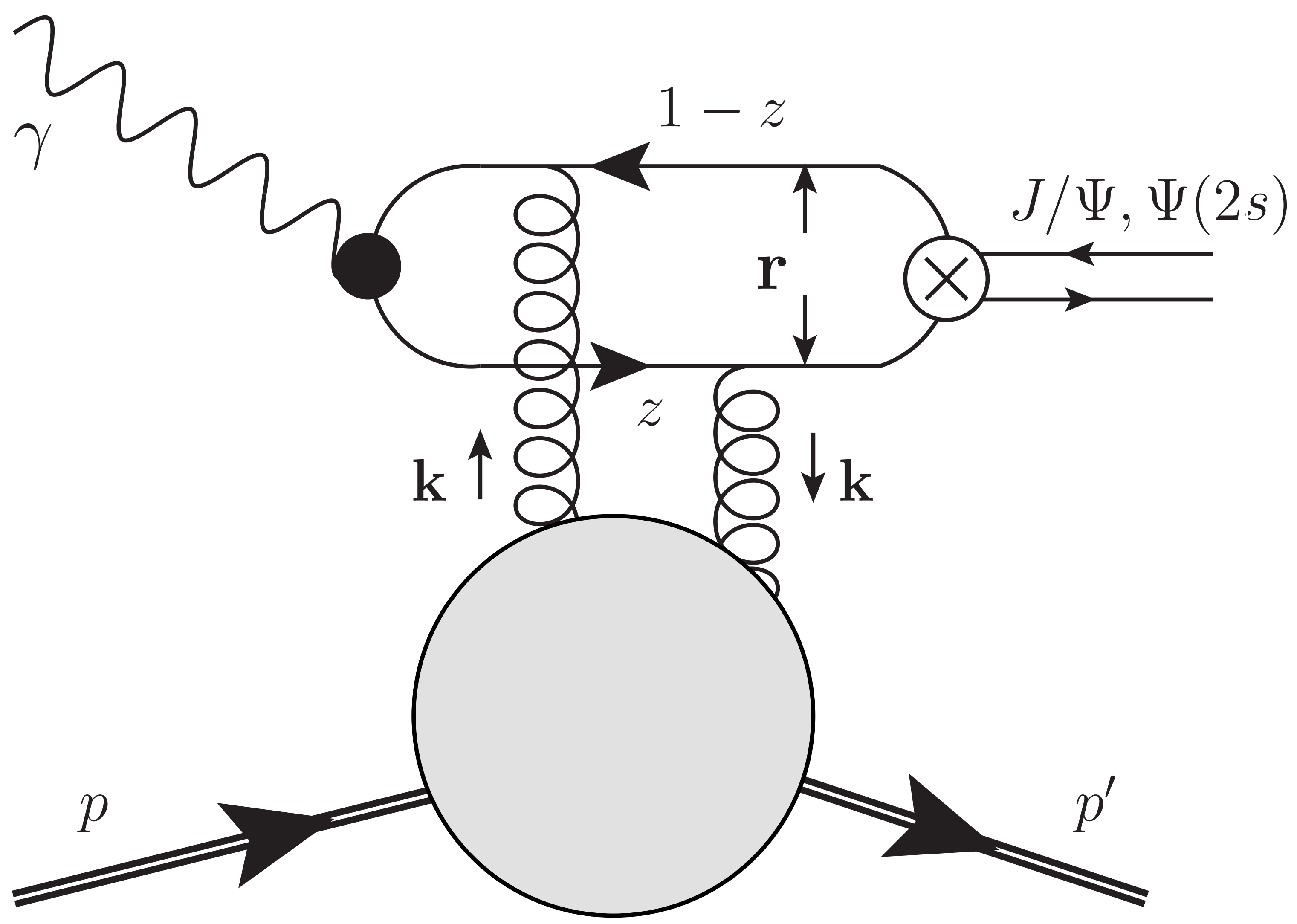

- J/Ψ: theory uncertainty bands due not allow to clearly distinguish between linear (stabilized) and non-linear evolution → reduction of uncertainty bands is needed
- $\Psi(2s)$: fixed scale HSS gluon suffers instability; stabilized HSS and KS gluon too close to distinguish them
- ratio: find different energy dependence for BFKL and BK gluon
[M. Krelina, J. Nemchik, R. Pasechnik, J. Cepila; 1901.02664] see decreasing ratio for Υ at the level of dipole models

- despite of all of its challenges: VM production remains a useful observable to quantify presence of non-linear effects in low x evolution equations
- probes different aspects (& suffers different uncertainties) than e.g. angular de-correlation dihadron or dijet → complementary observables

Appendix

the transition photon → quark-antiquark dipole → vector meson: Gaussian model

$$W(r) = 2\pi r \int_0^1 \frac{dz}{4\pi} \, (\Psi_V^* \Psi)_T(r,z)$$

$$(\Psi_V^* \Psi)_T \, (r,z) = \frac{\hat{e}_f e N_c}{\pi z(1-z)} \left\{ m_f^2 K_0(\epsilon r) \phi_T(r,z) - \left[z^2 + (1-z)^2\right] \epsilon K_1(\epsilon r) \partial_r \phi_T(r,z) \right\}$$

boosted Gaussian scalar wave function using Brodsky-Huang-Lepage prescription

$$\phi_{T,L}^{1s}(r,z) = \mathcal{N}_{T,L} z(1-z) \exp\left(-\frac{m_f^2 \mathcal{R}_{1s}^2}{8z(1-z)} - \frac{2z(1-z)r^2}{\mathcal{R}_{1s}^2} + \frac{m_f^2 \mathcal{R}_{1s}^2}{2} \right)$$

parameters from normalization and decay width **[Armesto, Rezaeian; 1402.4831]** (J/Ψ) and **[Goncalves, Moreira,Navarra;1408.1344]** (ϒ)

Meson	m_f/GeV	$\mathcal{N}_T$	$\mathcal{R}^2/\mathrm{GeV}^{-2}$	M_V/GeV
J/ψ	$m_c = 1.4$	0.596	2.45	3.097
Υ	$m_b = 4.2$	0.481	0.57	9.460